

Aspartic acid scaffold in bradykinin B1 antagonists

József Huszár,^{a*} Zoltán Timár,^a Ferenc Bogár,^b Botond Penke,^{a,b} Róbert Kiss,^c Krisztina Katalin Szalai,^c Éva Schmidt,^c Andrea Papp^c and György Keserű^c

Several novel bradykinin B1 receptor (B1R) antagonists were synthesized utilizing a new aspartic acid scaffold. This core is derived from the highly potent dihydroquinoxalinone scaffold published recently by researchers at Merck (Ha *et al. Biochem. Biophys. Res. Commun.* 2005, 331, 159–166). Despite the considerably limited chemical space of B1 antagonists, the synthesized compounds still showed significant biological activity. None of the four most potent compounds showed significant activity on the bradykinin B2 receptor (B2R), consequently they can be considered as valuable starting points for designing more potent and selective B1 antagonists. Furthermore, the synthesis of these aspartic acid derivatives is much simpler than that of the original Merck compounds suggesting efficient parallel synthesis approaches during their optimization. Docking known and novel B1 antagonists into the refined B1R homology model including the second extracellular loop (EC2) underlined the importance of this loop in ligand binding. Comparative binding mode analysis revealed that our novel compounds bind similar to the dihydroquinoxalinone template. Our results indicate that the rigid core of the dihydroquinoxalinone containing B1 antagonists is not crucial for maintaining B1 activity. Copyright © 2009 European Peptide Society and John Wiley & Sons, Ltd.

Keywords: bradykinin; B1 antagonists; peptidomimetic; binding modes; docking

Introduction

Despite the large number of available analgesics, chronic pain is still in the focus of pharmaceutical research and development. Although acute pain killers can be used effectively, chronic pain remains a significant unmet medical need. The most frequently used chronic medications are nonsteroidal anti-inflammatory drugs (NSAIDs) and opioid analgesics. These two classes of drugs possess, however, serious side effects [1] that make them suboptimal for long-term treatment.

Kinins are oligopeptide hormones referring to two endogenous peptides: BK (amino acid sequence: RPPGFSPFR) and kallidin (Lys-BK) (amino acid sequence: KRPPGFSPR). BK and Lys-BK are produced through proteolytic cleavage of high- and low-molecular weight kininogen precursor proteins, respectively. This cleavage is realized by plasma and tissue serine proteases, called kallikrein enzymes [2,3]. The most important physiological effects of kinins are vasodilatation, increased vascular permeability, vascular and bronchial smooth muscle contraction, stimulation of sensory neurons, alteration of ion secretion of epithelial cells, renal homeostasis, production of nitric oxide, release of prostaglandins and cytokines [4–6]. Pathological overproduction of kinins was observed in several disorders, such as hyperalgesia, hypotension, sepsis, pancreatitis, brain edema, and a wide variety of immunological and inflammatory diseases (e.g. asthma, rheumatoid arthritis, and multiple sclerosis) [4].

The physiological effects of kinins are mediated by BK receptors. These are members of the G protein-coupled receptor (GPCR) superfamily. GPCRs are transmembrane (TM) receptors and consist of seven TM helices as well as a short eight helix that runs parallel with the cytoplasmic surface. The highly conserved tertiary structure makes it possible to build relevant homology models of

GPCRs. Until recently, these models were primarily based on the crystal structure of bovine rhodopsin (BR) first solved by Palczewski *et al.* [7] in 2000. At the end of 2007, however, the first GPCR crystal structures of the human β_2 -adrenergic receptor (h β_2 AR) were published [8,9]. These novel GPCR crystal structures are believed to be specifically useful for developing novel GPCR homology models, especially in the case of aminergic GPCRs. For other GPCRs, however, the choice of the template (i.e. BR or h β_2 AR) should be founded on the homology between the target protein and the available templates.

On the basis of the pharmacological differences, BK receptors can be classified as B1 and B2 receptors (B1R and B2R) [5,6]. Kinins (BK and Lys-BK) are selective endogenous agonists of B2R. High levels of B2R are expressed in a wide variety of tissues related to acute cellular responses. B2R is primarily located on nociceptive neurons as well as in the cardiovascular system. Activators of B2R have long been known to induce acute inflammatory pain. In contrast, C-terminally truncated des-Arg carboxypeptidase metabolites of BK (des-Arg9-BK) and Lys-BK (des-Arg10-kallidin) are selective B1 ligands. B1R is only expressed in low levels under

* Correspondence to: József Huszár, Department of Medical Chemistry, University of Szeged, Dóm tér 8., H-6720, Szeged, Hungary.
E-mail: huszarjosef@yahoo.com

a Department of Medical Chemistry, University of Szeged, Dóm tér 8., H-6720, Szeged, Hungary

b Supramolecular and Nanostructured Materials Research Group of the Hungarian Academy of Sciences, University of Szeged, Dóm tér 8., H-6720, Szeged, Hungary

c Gedeon Richter Plc., Gyömrői út 19-21., H-1103, Budapest, Hungary

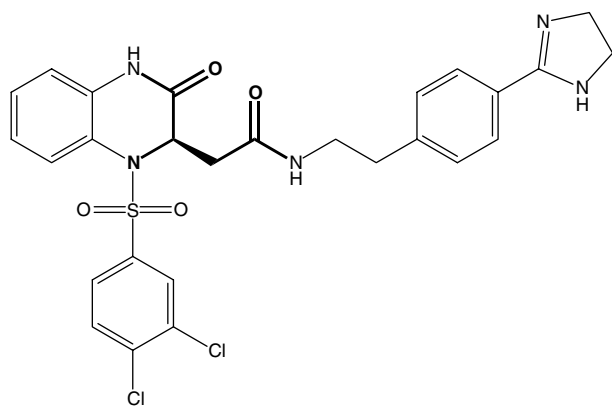


Figure 1. A highly potent dihydroquinoxalinone core based B1 antagonist (**M2**) from ref. 33 including the D-aspartic acid derivative as a scaffold (**bold**).

normal conditions, but the expression is considerably induced locally by inflammation, tissue injury, or trauma [10]. Under inflammatory conditions, a shift of kinin receptor expression from B2R to B1R has been reported in both *in vitro* and *in vivo* models [11,12]. Functionally active B1Rs were newly expressed, whereas B2R expression was significantly decreased following peripheral nerve injury in mice [12]. Siebeck *et al.* [13] found a significant induction of B1R expression using noxious stimuli not only in healthy animals but also in animals with a pre-existing infection. The role of B1R in inflammatory diseases is further supported by the considerable upregulation of B1R found in a mouse model of colitis [14]. In another study, Stadnicki *et al.* [15] showed that B1R expression in epithelial cells is significantly increased in human intestinal inflammation. Moreover, in the comprehensive review of Duchene and Ahluwalia [16] it was established that the endothelial B1R activation is a crucial step in the progression of inflammatory cardiovascular disease.

Over the last decade, growing evidence has implicated an important role for B1R in chronic pain associated with inflammatory conditions [2,17,18]. Consequently, B1R is a promising drug target; potent, selective, and orally available B1 antagonists may possess significant therapeutic potential in chronic pain [19].

Highly potent and selective peptide and nonpeptide B2 agonists and antagonists are already available. On the other hand, nonpeptide B1 ligands were first reported in the past few years only [19,20]. After the discovery of the first class of peptide B1 antagonists [4,21], several further peptide [19] and pseudopeptide [1,22] B1 antagonists were published. Peptide B1 antagonists are useful for the biological characterization of B1R. They can, however, hardly become drug candidates because of their generally poor pharmacokinetics. On the other hand, nonpeptide B1 antagonists can be considered as promising analgesics suitable for oral administration. Very recently, nonpeptide B1 antagonists have been reported as potent analgesic agents [23–29]. B1 antagonists containing rigid scaffolds such as benzodiazepine have been identified with an *in vivo* analgesic effect comparable to that of morphine in a number of hyperalgesia models [29,30]. A series of 2,3-diaminopyridines [31] and 2-alkylamino-5-sulfamoylbenzamides [1] were also reported as potent B1 antagonists. Incorporation of piperidine 3- and 4-carboxylic acid spacers and the introduction of morpholine and piperazine groups increased B1 binding affinity and oral absorption in animal models significantly [1].

Researchers at Merck reported highly potent and selective arylsulfonamide dihydroquinoxalinone B1 antagonists in four different papers [23,30,32,33]. One representative compound (Figure 1) (**M2**) of this series showed excellent B1 affinity [human bradykinin B1 receptor (hB1R) $K_i = 0.03$ nM]. Docking simulations on the homology model of the hB1R suggested that the phenylsulfonamide moiety of **M2** plays a key role in receptor binding. Structural analysis of a broad set of B1 antagonists also indicates that the phenylsulfonamide moiety is important for maintaining B1 affinity.

Since the number of B1 antagonists discovered so far is still considerably low, novel scaffolds possessing B1 activity can be of high importance. In this report, a ligand-based approach has been utilized to design and synthesize a series of novel, nonpeptide B1 antagonists. As the dihydroquinoxalinone core includes a D-aspartic acid derivative (see Figure 1), we introduced a series of D- and L-aspartic acid esters and amides for scaffold hopping. In this orthogonal (one-factor-at-a-time) experiment, all of the synthesized compounds contained the crucial phenylsulfonamide moiety and modifications were restricted to the α -carboxyl and β -carboxyl functional groups (Figure 2). The primary goal of our study was to identify a novel scaffold with significant B1 affinity that can be used for developing new, potent and selective B1 antagonists.

Results and Discussion

Based on the dihydroquinoxalinone scaffold, we synthesized a series of compounds containing either α - or β -cyclohexyl/benzyl esters to test their B1 activity. As mentioned earlier, the phenylsulfonamide moiety is crucial for maintaining B1 affinity; therefore, all of the generated analogs carried the tosyl (4-toluenesulfonyl) sulfonamide moiety at the amino group. The free carboxyl function was transformed to corresponding amide using four different amines: 1,4-diaminobutane, 1,4-diaminohexane, agmatine, and 2-[4-(4,5-dihydro-1H-imidazol-2-yl)phenyl]ethylamine (imidazolyl-phenylethylamine). Using the L-aspartic acid core, compounds containing flexible alkyl side chains with a terminal primary amino group were synthesized for both the α - (**4,5**) (Scheme 1) and the β -cyclohexyl esters. (**14,15**) (Scheme 2). Further amines with a flexible alkyl linker and a terminal guanidine group were generated using either α -cyclohexyl (**6**) or α -benzyl esters (**7, 8**) (Scheme 1). In the case of the α -benzyl esters, both L- and D-aspartic acids were synthesized. Imidazolyl-phenylethylamine was applied for five further compounds using L-aspartic acid α -cyclohexyl ester (**9**) or α -benzyl ester (**10**), D-aspartic acid α -benzyl ester (**11**) (Scheme 1), L-aspartic acid β -cyclohexyl ester (**16**), and D-aspartic acid β -benzyl ester (**17**) (Scheme 2).

All of the synthesized compounds were then tested in a fluorometric human B1 Ca^{2+} assay. Compounds with primary alkyl amines or guanidine alkyl amines did not show B1 activity higher than 50% at a concentration of 5 μ M (see compounds **4, 5, 6, 7, 8, 14, and 15** in Table 1). Therefore, these compounds were not investigated any further. On the other hand, we found significant activity where the aspartic acid cores were attached to imidazolyl-phenylethylamine (see compounds **9,10,11,16, and 17** in Table 1). Compounds possessing a functional inhibition above 60% were further characterized in terms of hB1R binding affinity by a radioligand binding assay. K_i values of compounds **10, 16, and 17** were found to be in the low micromolar range. Moreover, compound **11** possessed a submicromolar K_i value. Interestingly,

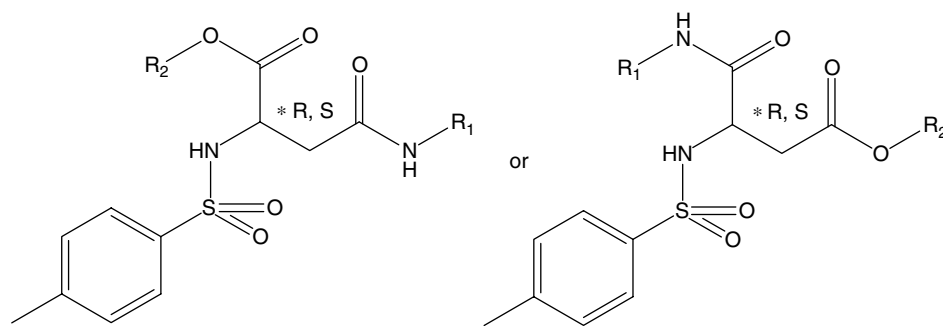
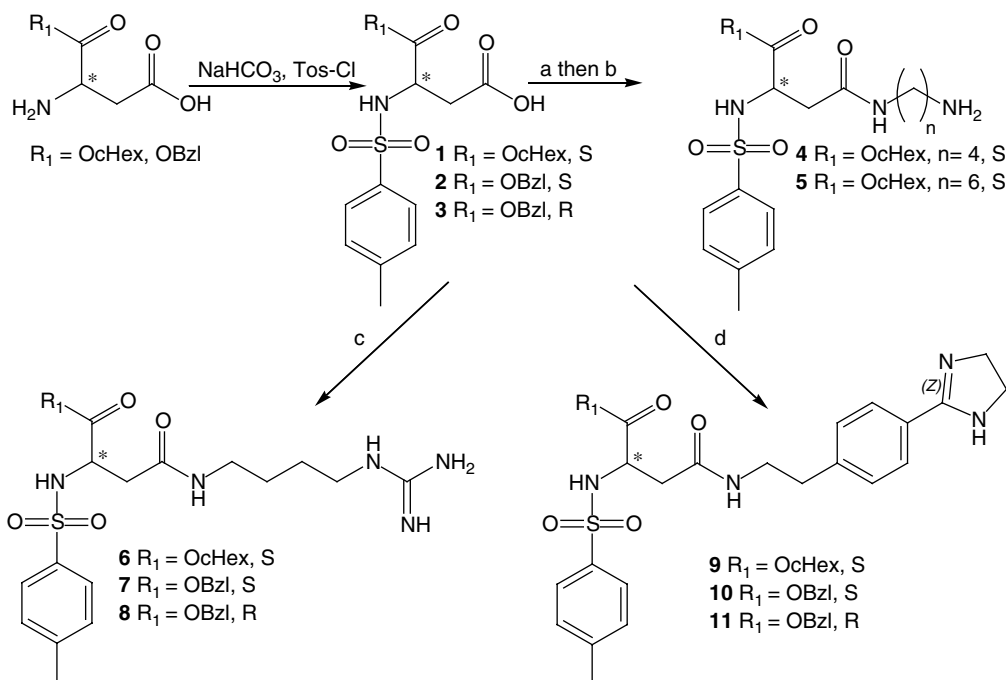


Figure 2. Tosylated aspartic acid cores, R_1 = basic amide side chain and R_2 = cHex or Bzl.



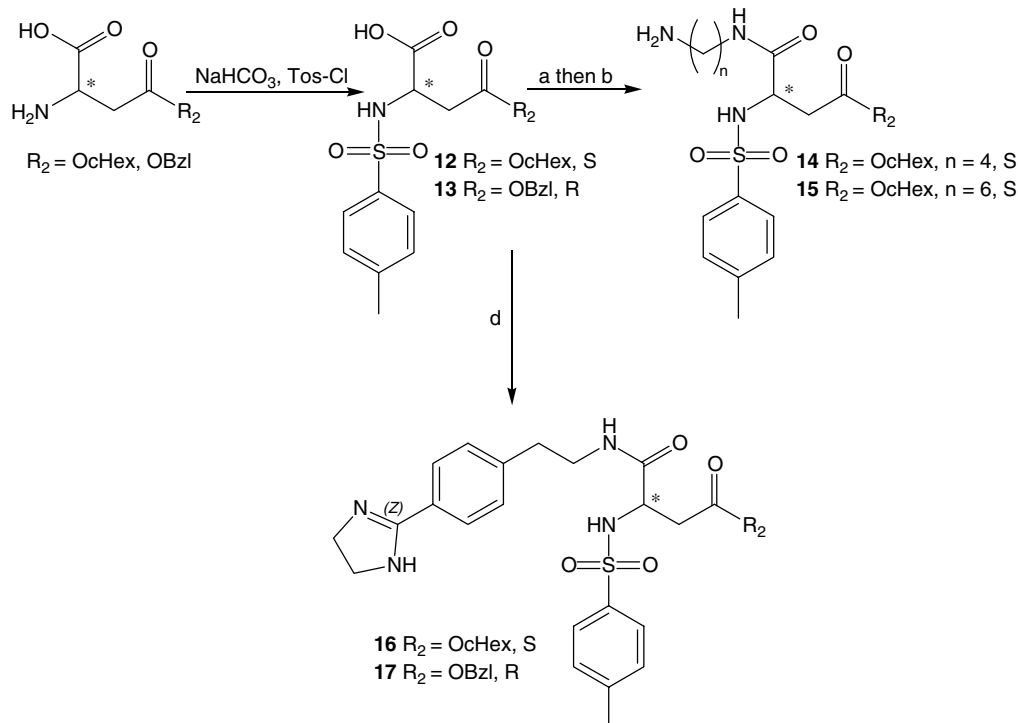
Scheme 1. Synthesis of B1 antagonists from aspartic acid α -esters. (a) DCC/HOBt, (4-amino-butyl)-carbamic acid tert-butyl ester or (6-amino-hexyl)-carbamic acid tert-butyl ester in DMF; (b) TFA/DCM; (c) HBTU/HOBt/DIEA in DMF (agmatin was used dissolved in aq. NaHCO_3); (d) HBTU/HOBt/DIEA, 2-[4-(4,5-Dihydro-1H-imidazol-2-yl)-phenyl]-ethylamine in DMF.

changing the position of the cyclohexyl ester ($\alpha \rightarrow \beta$) and the imidazolyl-phenylethylamine ($\beta \rightarrow \alpha$) resulted in a remarkable increase of B1 activity (53 and 102% for compounds **9** and **16**, respectively). Replacing the cyclohexyl group to benzyl also increased the B1 activity significantly (53 and 75% for compounds **9** and **10**, respectively). Changing the configuration of the aspartate from L to D in compound **10** yielded the most potent compound of this series with a human B1 binding K_i of $0.3 \mu\text{M}$ (compound **11**). According to these results, the D configuration of the aspartate and a benzyl group in α position were found as the most favored features. Interestingly, compound **17**, where the aspartate is also in D configuration but the position of the α - and β -substituents are switched, showed significantly lower B1 affinity than compound **11**. Comparing the compounds **10** and **17**, both the α - and the β -substituents and the chirality of the aspartic acid are inverted, therefore their substituents get into similar positions. This is in agreement with the fact that these two compounds possess similar B1 binding affinities ($K_i = 1.7$ and $2.1 \mu\text{M}$ for compounds **10** and **17**, respectively). We also analyzed the selectivity of the most potent compounds (**10**, **11**, **16**, and **17**) over the human

B2R in terms of functionality. None of the tested compounds exhibited inhibition higher than 10% in $5 \mu\text{M}$ concentration in the fluorometric human B2R Ca^{2+} assay (data not shown). These results suggest that our novel B1 antagonists are selective over the human B2R. Consequently, they can serve as chemical starting points for further optimization to develop highly potent B1 antagonists with sufficient selectivity in future.

Binding Mode of the Most Potent B1 Antagonists

After the synthesis and biological testing of our compound series, we were interested to investigate binding modes of these compounds within the hB1R binding pocket. In 2005, researchers at Merck published the first BR-based homology model of the hB1R [33]. The authors investigated the binding mode of several B1 antagonists of the dihydroquinoxalinone class (denoted as **M1–M9** below) using automated docking together with site-directed mutagenesis data. It was pointed out that residues in TM1, TM3, TM6, and TM7 were incorporated in forming the binding site of the hB1R. As the described model in complex with **M2** (referred



Scheme 2. Synthesis of B1 antagonists from aspartic acid β -esters. (a) DCC/HOBt, (4-amino-butyl)-carbamic acid tert-butyl ester or (6-amino-hexyl)-carbamic acid tert-butyl ester in DMF; (b) TFA/DCM; (d) HBTU/HOBt/DIEA, 2-[4-(4,5-Dihydro-1H-imidazol-2-yl)-phenyl]-ethylamine in DMF.

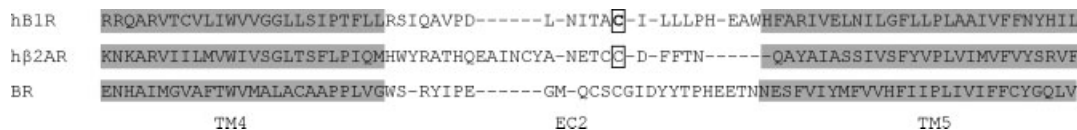


Figure 3. Sequence alignment of human B1R, h β 2AR, and BR in the region of TM4, TM5, and EC2.

as Merck model below) is available from the supplemental material of ref. 33, we decided to investigate the binding modes of our new ligands based on aspartic acid scaffold using this receptor model.

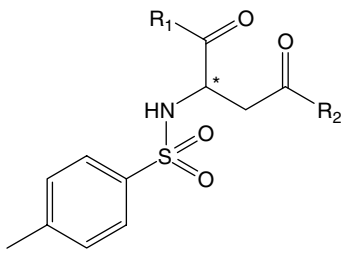
Unfortunately, it turned out that the published Merck model is not suitable for this purpose at its initial form, as it did not include the second extracellular loop (EC2). Recent studies pointed out the importance of EC2 for the proper functioning of GPCRs. Raganathan [34] emphasized the possible role of EC2 in ligand selectivity. Moreover, Massotte *et al.* [35] suggested that EC2 may stabilize the inactive conformation of the receptor and controls the on-off transition. Site-directed mutagenesis data combined with molecular modeling revealed that amino acids Pro182 (EC2) and Leu192 (EC2) of the hB1R interact with the [Leu⁹]DesArg¹⁰ kallidin peptide B1 antagonist [36]. These representative results demonstrate the importance of a well-established EC2. Consequently, we decided incorporating EC2 into our model. As the Merck model was based on the structure of BR [7] (PDB ID: 1F88), we used this template constructing EC2.

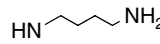
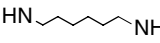
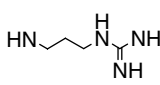
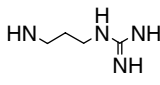
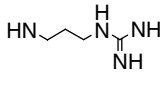
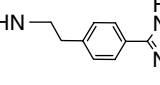
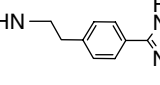
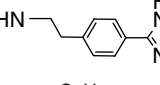
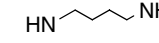
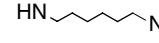
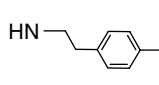
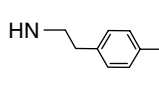
Homology modeling was started from the sequence alignment published in ref. 33 to build up the complete hB1R structure using Modeller (version 9.5) [37]. As a next step, this model was aligned with the Merck model and EC2 was transferred to the original Merck model. After that, the modified Merck model including EC2 was refined by simulated annealing and subsequent minimizations.

The most recent X-ray structure of h β 2AR was published by Hanson *et al.* [38] in 2008 (PDB ID: 3D4S). Since EC2 of BR and

h β 2AR possess a fundamentally different structural fold (BR: β -sheet, h β 2AR: α -helix), we also generated a model for EC2 using the crystal structure of h β 2AR. The sequence alignment between B1R, h β 2AR, and BR generated by ClustalW (version: 2.0.10.) revealed that B1R is phylogenetically closer to BR (data not shown). This would suggest BR to be a more suitable template for B1R homology modeling. In agreement with this finding, we found that B1R shows significantly lower homology to h β 2AR than to BR in EC2 (Figure 3). In particular, h β 2AR contains a disulfide bridge between Cys184 (EC2) and Cys190 (EC2), which appears neither in BR nor in B1R. Cys191 (EC2) in h β 2AR forms another disulfide bridge with Cys106 (EC1). This disulfide bridge also exists in B1R formed by Cys110 (EC1) and Cys189 (EC2). Consequently, Cys189 (EC2) in B1R and Cys191 (EC2) in h β 2AR have to be aligned with each other (see boxed C residues in Figure 3). This constraint implies the insertion of gaps both in B1R and h β 2AR. These gaps do not appear in the alignment of B1R and BR (see Figure 3), this way B1R shows higher similarity to BR than to h β 2AR in the EC2 region. Nevertheless, we built up another B1R model including EC2 based on the h β 2AR template.

Figure 4 shows the two EC2 loop structures obtained by using BR as well as h β 2AR as a template. The binding positions of the highly active **M2** ligand are also shown. The loop obtained from the BR reaches the binding pocket and forms several interactions with the bound **M2** (see the details below). The loop model based on h β 2AR stays away from the binding region.

Table 1. Biological assay results using Chinese hamster ovary cells expressing human B1 receptors (CHO-hB1). N.D.: not determined


	R1	R2	Relative config.	[Ca ²⁺] _i assay CHO-hB1 Inhibition (%) at 5 μM	Binding assay CHO-hB1 K _i (μM)
4	OcHex		L	<50 %	N.D.
5	OcHex		L	<50 %	N.D.
6	OcHex		L	<50 %	N.D.
7	OBzl		L	<50 %	N.D.
8	OBzl		D	<50 %	N.D.
9	OcHex		L	53%	N.D.
10	OBzl		L	75%	1.7
11	OBzl		D	98%	0.3
14		OcHex	L	<50 %	N.D.
15		OcHex	L	<50 %	N.D.
16		OcHex	L	102%	1.7
17		OBzl	D	95%	2.1

To test the quality of the EC2 loops based on BR and h β_2 AR, we docked the **M1–M9** ligands to both receptor models with the FlexiDock program implemented in the SYBYL 7.3 package [39]. Docking scores obtained for **M1–M9** ligands in the BR-based receptor model *versus* B1R affinity values are presented in Figure 5 (filled squares ■). The measured binding affinities and the calculated FlexiDock scores show similar correlation to that of obtained by Ha *et al.* [33]. The correlation in the h β_2 AR-based model is significantly lower ($r^2 = 0.53$ after linear fitting) than in the BR-based one ($r^2 = 0.84$); therefore, we concluded that the latter model is in a better agreement with the available experimental data. Therefore, we present docking results obtained with the BR-based model only in the remaining part of the manuscript.

Figure 6 reports the binding mode of the imidazolyl-phenylethylamine ligand (**M2**). H-bonds were identified using geometrical criteria as (i) the distance of acceptor and the H atom is not larger than 2.8 Å and (ii) the donor-H-acceptor angle is not smaller than 120°. In agreement with the high B1R binding affinity, we could identify several H-bonds between **M2** and the receptor: (i) one of the oxygens of the sulfone group with the OH group of Trp98 (2.65 – Ballesteros-Weinstein numbering [40]), the other oxygen with Gln295 (7.36); (ii) the protonated nitrogen of the imidazolyl-phenylethylamine chain with one of the carboxylate oxygens of Glu273 (6.59); (iii) the oxygen atom of the core with the side chain amine group of Asn114 (3.29); (iv) the oxygen of the ligand's amide group with Asn114 (3.29); (v) the



Figure 4. EC2 loop structures of B1R generated by using BR (green) and $h\beta_2$ AR (yellow) as templates. The binding positions of **M2** are shown in red (BR-based EC2) and gray ($h\beta_2$ AR-based EC2).

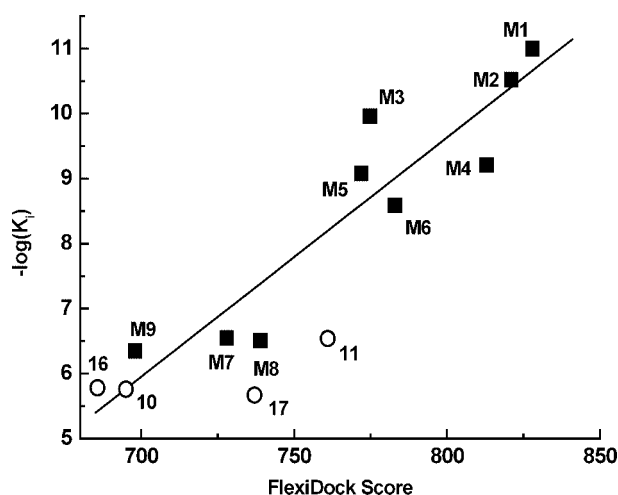


Figure 5. Correlation between the experimental binding affinity $-\log(K_i)$ and the scores obtained from docking to our BR-based receptor model with FlexiDock for ligands **M1–M9** (■) as well as for the new active compounds **10**, **11**, **16**, and **17** (○). Linear regression ($r^2 = 0.84$) for the data of **M1–M9** ligands is also shown (solid line).

NH of the same amide group with Asn298 (7.39); and (vi) the backbone carbonyl oxygen of Ile113 (3.28) with the NH of the core. The dihydroquinoxaline group is located in the hydrophobic pocket (HP1) formed by residues Phe302 (7.42) and Ile113 (3.28). The lipophilic dichlorobenzene ring is positioned in a second hydrophobic pocket (HP2) formed by Trp103 (EC1) and Ile186 (EC2). The lipophilic part of the imidazolyl-phenylethylamine chain interacts with the lipophilic side chains of Ala188 (EC2), Ile190 (EC2), and Leu294 (7.35) (HP3). **M2**, on the other hand, did not occupy another hydrophobic pocket formed by Phe302 (7.42) and Ile117 (HP4) (see Figure 6).

After analyzing the binding mode of **M2**, we docked our novel active ligands (**9**, **10**, **11**, **16**, and **17**; see Table 1) with FlexiDock to the binding site. In Figure 7, the binding poses and H-bonds of the investigated ligands are presented and compared to that of **M2**. Interestingly, our ligands showed a similar binding mode to that of **M2**, suggesting that our approach was successfully applied for scaffold hopping. The imidazoline amine group of

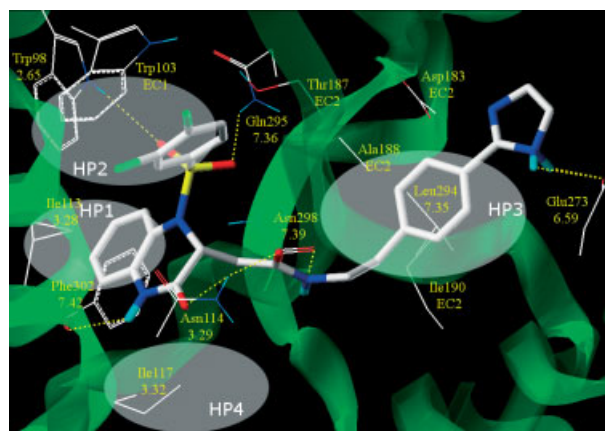


Figure 6. Binding conformation of **M2** and the H-bonds (dashed yellow lines) formed between the ligand and the receptor. The hydrophobic regions (HP1–HP4) are indicated by dashed violet ellipses. Only the side chains of the closest amino acids are shown.

each investigated ligand formed an H-bond with Asp183 (EC2) and Glu273 (6.59), except compounds **9** and **10** where only the interaction with Asp183 (EC2) fulfilled the geometrical criteria of the H-bonds. These two ligands (**9** and **10**) showed the lowest biological activity (53.1 and 75.4% functional inhibition in $[Ca^{2+}]_i$ assay, respectively). This finding underlines the importance of the interaction between the imidazolyl-phenylethylamine chain and Glu273 (6.59). We speculate that the lower performance of compound **9** stems from the minor structural difference between **9** and **10** ($R_1 = \text{OCHex}$ or OBzl , respectively), namely the complementarity of the OCHex group to HP1 is suboptimal; however, it forms interactions with HP4. Moreover, we found that compound **10** occupied a similar binding mode to that of **M2** by fitting its OBzl group more favorably to HP1. This is also in agreement with the H-bond pattern of compound **10**, which is more similar to that of **M2** by forming H-bonds with Asn114 (3.29) and Asn298 (7.39) simultaneously (Figure 7B).

Compound **11** is the enantiomer of **10**. This modification (L \rightarrow D) of the core allowed the formation of two additional H-bonds between the sulfone group and Gln295 (7.36) as well as between the imidazoline amine group and Glu273 (6.59) (Figure 7C). This resulted in the highest binding affinity as well as the best FlexiDock score of the novel ligands (see Figure 5).

Exchanging the R_1 and R_2 groups of **9** we obtained compound **16**. The displacement of the imidazolyl-phenylethylamine chain to the R_1 position improved the affinity significantly. The most important H-bonds in this case are formed by the protonated nitrogen at the end of the imidazolyl-phenylethylamine chain with Glu273 (6.59) and Asp183 (EC2) (Figure 7D). The binding position of the two lipophilic rings was interchanged, i.e. the OCHex group of compound **16** sits in HP2 and the tosyl group in HP4 that allows the formation of only one further H-bond between the core and Asn114 (3.29) leading to a poor FlexiDock score (see Figure 5).

The ligand **17** was derived from **11** in the same way as **16** could from **9**, by exchanging the R_1 and R_2 groups. In this case, however, the B1 activity decreased. The H-bonds formed by **17** are similar to that of **11**, but the positioning of the lipophilic OBzl group is different: it was found in HP1 (similarly to the aromatic ring of the core in **M2**) and not in HP4 as in the case of compound **11** (see Figure 7E).

Our results showed that the protonated nitrogen in the imidazoline ring of the imidazolyl-phenylethylamine chain plays a

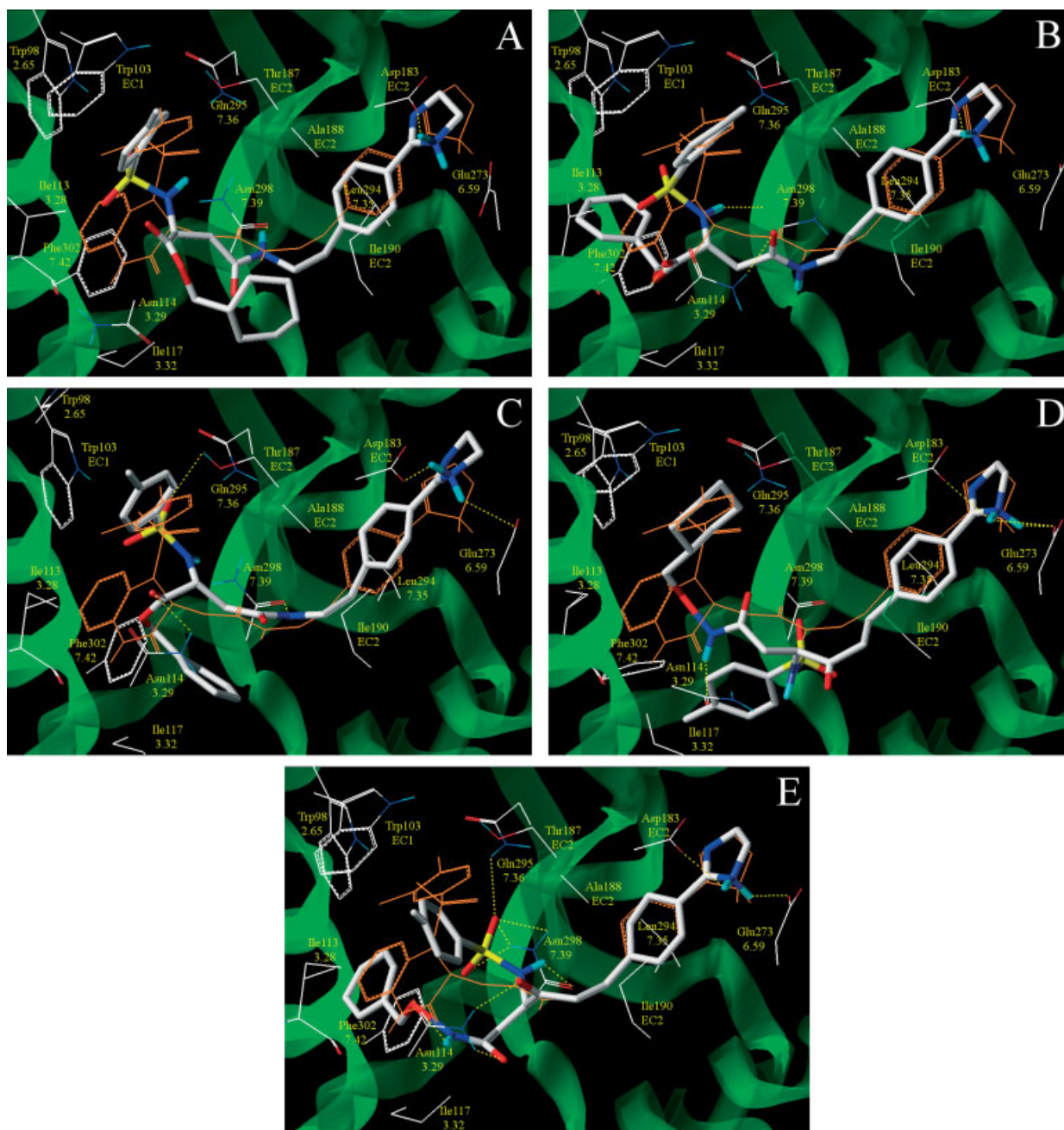


Figure 7. Binding pose of the active ligands [9 (panel A), 10 (panel B), 11 (panel C), 16 (panel D), and 17 (panel E)] compared to that of **M2** (orange).

crucial role in the interaction with the binding site for **M2** as well as for our novel compounds. On the other hand, strong hydrophobic interactions between the rings of the ligands and the lipophilic pockets of the receptor were also identified.

Conclusion

In conclusion, we have synthesized several novel B1 antagonists utilizing a new aspartic acid scaffold. This core is derived from the previously described dihydroquinoxalinone scaffold of Merck. Despite the considerably limited chemical space of B1 antagonists, the synthesized compounds still showed significant biological activity in a functional B1R Ca^{2+} assay, therefore

they can be considered as valuable starting points for further optimization. None of the four most potent compounds showed significant B2 activity that further indicates the usefulness of these compounds for designing more potent and selective B1 antagonists. Furthermore, the synthesis of these aspartic acid derivatives is much simpler than that of the original Merck compounds suggesting efficient parallel synthesis approaches during their optimization. We have modified the previously published B1R model of Ha *et al.* [33] by including EC2 based on the BR crystal structure. Docking calculations pointed out the importance of EC2 in ligand binding and revealed that the binding mode of the novel compounds is similar to that of the dihydroquinoxalinone template molecule. In addition to the successful scaffold hopping, our results also highlighted that

the rigid core of the published B1 antagonists is not crucial for maintaining B1 activity.

Experimental

Fluorometric Measurement of Cytoplasmic Ca^{2+} [Ca^{2+}]_i

All materials and cell culture reagents were from Invitrogen (Carlsbad, CA, USA) and Sigma-Aldrich (St Louis, MO, USA), the hB1R expressing cell line was purchased from Euroscreen (Belgium). For the [Ca^{2+}]_i measurements, we used Chinese hamster ovary (CHO) cells stably expressing recombinant hB1Rs. Cells were cultured in Dulbecco's modified Eagle medium containing 10% foetal bovine serum, 1% MEM nonessential amino acid solution, and 400 µg/ml G418 and antibiotics (0.25 µg/ml amphotericin B, 100 U/ml penicillin G, 100 µg/ml streptomycin). Cells were kept at 37 °C in a humidified atmosphere of 5% CO₂/95% air. Cells were plated into 96-well microplates at a density of 2.5×10^4 cells/well and measurements of [Ca^{2+}]_i were carried out 1 day after cell plating. After removing the medium, cells were loaded with a calcium-sensitive fluorescent dye, fluo-4 (2 µM), for 40–120 min in the following buffer: 2 mM MgCl₂, 140 mM NaCl, 5 mM KCl, 5 mM HEPES-Na, 5 mM HEPES, 2 mM CaCl₂, 20 mM d-glucose, and 2 mM probenecid. To remove excess dye, cells were washed twice with buffer. After washing, the test compounds were added and the cells were incubated for 20–25 min at 37 °C. The test compounds were diluted in buffer from a DMSO stock solution, final DMSO concentration was <0.1%. After the incubation period, baseline and agonist-evoked fluorescence changes were monitored with a plate reader fluorometer (Fluoroskan Ascent, Thermo-Labsystems, Finland). The agonist was [Lys-des-Arg9]-BK applied at an EC₈₀ concentration. Excitation was at 485 nm, detection of fluorescence emission was carried out at 538 nm. The whole measurement process was performed at 37 °C and was controlled by custom software. Raw fluorescence data were expressed as ΔF/F values (fluorescence change normalized to baseline). Inhibitory effect of the test compounds was expressed as percent inhibition of the control agonist response. Data analysis was carried out with Microsoft Excel.

Human Recombinant Bradykinin B1 Receptor Binding Assay

Preparation of membrane

Membrane was prepared from hB1-A5 cells (expressed in CHO cells) according to the Euroscreen Technical Data Sheet (Cat. No.: ES-091). Cells were dissociated in Dulbecco's phosphate buffered saline (DPBS) and centrifuged (1500 rpm, 10 min, 4 °C). The pellet was resuspended in 15 mM Tris-HCl pH 7.5, 2 mM MgCl₂, 0.3 mM EDTA, 1 mM EGTA, and homogenized in a glass homogenizer. The crude membrane fraction was collected by two consecutive centrifugation steps at 40 000 g for 25 min at 4 °C separated by washing step in above-described buffer. The final pellet was resuspended in buffer 75 mM Tris-HCl pH 7.5, 12.5 mM MgCl₂, 0.3 mM EDTA, 1 mM EGTA, and 250 mM sucrose. Membrane was divided into aliquots, flash frozen, and stored at –80 °C until use. Protein concentration was determined using the BCA method.

Binding conditions

Binding assays were performed in triplicate in DeepWell plates containing the binding buffer (50 mM Tris-HCl pH 7.4, 5 mM MgCl₂), hB1 membrane (20 µg protein/tube), [³H] Kallidin (Perkin

Elmer Life Sciences) as radioligand. Nonspecific binding was determined in the presence of 10 µM Lys-des-Arg⁹-BK. The samples were incubated in a final volume of 0.25 ml for 15 min at 25 °C. Binding reactions were terminated by rapid filtration through 96-well GF/B Unifilter presoaked for at least 1 h in 0.5% PEI. Filters were washed four times with 1 ml of ice-cold washing buffer (same composition as the binding buffer) using Brandel harvester. Filters were allowed to dry, Perkin Elmer Microscint 20 scintillant was added (20 µl/well), and bound radioactivity was determined by Packard TopCount scintillation counter for 3 min. Data were analyzed with Prism, Graph Pad Software.

Molecular Modeling

Homology modeling

The sequence alignment between B1R, hβ₂AR, and BR was generated by ClustalW (version: 2.0.10.). The 3D structure was built up using Modeller (version 9.5) [37].

Loop refinement

The B1R model obtained from ref. 33 was extended by EC2 loops extracted from the models created by Modeller. As a next step, the original parts of the receptor including the bound ligand were kept fixed and a simulated annealing protocol (1 ps equilibration at 700 K followed by a 10 ps exponential cooling to 200 K, repeated 10 times) and a subsequent energy minimization were carried out using Sybyl 7.3 [39]. Three representatives from the resulted 10 structures were selected. Keeping the ligand fixed, its 6 Å environment was relaxed in each case. Finally, the **M2** ligand was docked to these structures and the EC2 loop model with the best score was selected for further investigations.

Flexible docking

We docked nine reference B1 antagonists (**M1–M9**) as well as our novel ligands to the binding site by the docking program FlexiDock (SYBYL 7.3 package [39]). Residues closer than 6 Å to the docking position of **M2** were considered as the binding pocket. Bonds in the side chains of these residues were defined as rotatable for the flexible docking. The generation number in the genetic algorithm (GA) was set to 100 000, for the other parameters of GA we used the default values. The initial position and conformation of the ligands was chosen to overlap as favorably as possible with the docked **M2** molecule found in the Merck model.

Chemistry

Commercial chemicals and solvents were of reagent grade and used without further purification. The following abbreviations are used: DCC, N,N'-dicyclohexylcarbodiimide; DCM, dichloromethane; DIEA, ethyl-diisopropyl-amine; DCU, N,N'-dicyclohexylurea; DMF, dimethyl formamide; HBTU, 2-(1-H-benzotriazol-1-yl)-1,1,3,3-tetramethyluronium hexafluorophosphate; HOBt, 1-hydroxy-benzotriazol; and TFA, trifluoroacetic acid. Preparative reverse phase HPLC was performed on a Shimadzu SPD-6AV 3000 liquid chromatograph using a C18 reverse phase silica gel column (Phenomenex, Jupiter 258 × 21.2 mm, 15 µ, 300 Å). Eluent: acetonitrile (20–100%, v/v) in water containing 0.1% (v/v) TFA. Peak detection was at 254 nm. NMR: Bruker Avance DRX 500 Spectrometer (1H: 500.13 MHz), CDCl₃ or DMSO-d₆ solutions, δ (ppm), J (Hz). Spectral patterns: s, singlet; d, doublet; dd,

double doublet; t, triplet; and m, multiplet. High-resolution exact mass measurements were performed on a hybrid, quadrupole orthogonal acceleration time-of-flight mass spectrometer (Waters Q-ToF Premier), equipped with a nano electrospray ionization source. Samples were diluted with 0.1% formic acid (v/v) solvent to obtain optimal ion intensity for exact mass measurement. Measurements were performed immediately after calibration on mass spectral fragments of [Glu¹]fibrinopeptide (200 fmol/μl solution). All products were purified by preparative HPLC and co-freeze-dried. Amines were gained as trifluoroacetate salts. Lyophilized products were tested in biological assays without desalting or further purification. Chemical yields are not optimized.

Tos-Asp-OcHex-OH (1)

Boc-Asp-OcHex • DCHA salt was converted to the free acid. Boc-Asp-OcHex • DCHA (4.876 g, 9.82 mmol) was suspended in 40-ml ethyl acetate in a separating funnel. 1.2 equivalents of ice-cold 2 M H₂SO₄ was added and shake until dissolved. The separated aqueous layer was washed with 2 × 40 ml of ethyl acetate. The combined organic layer was washed with 2 × 20 ml of water, dried with Na₂SO₄, filtered and concentrated. The crude residue was dissolved in 50% TFA/DCM (5 ml), then the reaction mixture was stirred for 20 min at room temperature and then the solvent was removed *in vacuo* to give H-Asp-OcHex-OH (2.010 g, 9.34 mmol). This product was dissolved in distilled water (30 ml) and NaHCO₃ (1.569 g, 18.64 mmol) was added, followed by the dropwise addition of 4-methyl-benzenesulfonyl chloride (2.06 g, 10.81 mmol) in acetone (20 ml) then the reaction mixture was stirred at room temperature for 6 h at pH = 8. The acetone was removed under vacuum and the residue was extracted with NaHCO₃/diethyl ether (25 ml). The basic solution was acidified with solid NaHSO₄ to pH = 4–5 and extracted with ethyl acetate (3 × 10 ml). The combined organic phases were dried, filtered, and concentrated. The crude product was crystallized from ethyl acetate/diethyl ether and gave Tos-Asp-OcHex-OH (3.325 g, 9.00 mmol, 96%). HRMS (EI) Calcd for C₁₇H₂₃NO₆S *m/z*: 370.1324 (M + H). Found: *m/z* 370.1167 (M + H). 1H NMR (500 MHz, DMSO-*d*₆) δ 7.79 (2H, d, *J* = 8 Hz), 7.49 (2H, d, *J* = 8 Hz), 4.59 (1H, s), 4.22 (1H, s), 3.50 (1H, s), 2.73 (3H, m), 2.62 (3H, s), 1.73 (4H, m), 1.34 (6H, m).

Tos-Asp-OBzl-OH (2)

NaHCO₃ (1.680 g, 20.00 mmol) was added to a solution of H-Asp-OBzl-OH (2.232 g, 10.00 mmol) in distilled water (30 ml), followed by the dropwise addition of 4-methyl-benzenesulfonyl chloride (2.100 g, 11.01 mmol) in acetone (20 ml) then the reaction mixture was stirred at room temperature for 4 h at pH = 8. The acetone was removed under vacuum and the residue was extracted with NaHCO₃/diethyl ether (25 ml). The basic solution was acidified with solid NaHSO₄ to pH = 4–5 and extracted with ethyl acetate (3 × 20 ml). The combined organic phases were dried, filtered, and concentrated. The crude material was purified by flash chromatography on silica gel (25–50% ethyl acetate:hexanes gradient) to give Tos-Asp-OBzl-OH (634 mg, 1.68 mmol, 17%). HRMS (EI) Calcd for C₁₈H₁₉NO₆S *m/z*: 378.1011 (M + H). Found: *m/z* 378.0909 (M + H). 1H NMR (500 MHz, DMSO-*d*₆) δ 7.79 (2H, d, *J* = 8 Hz), 7.47 (5H, m), 7.39 (2H, d, *J* = 8 Hz), 5.03 (2H, dd, *J* = 12 Hz), 4.33 (1H, dd, *J* = 7 Hz), 3.51 (1H, s), 3.42 (2H, t, *J* = 7 Hz), 2.84 (3H, s), 2.66 (1H, s).

Tos-D-Asp-OBzl-OH (3)

NaHCO₃ (430 mg, 5.38 mmol) was added to a solution of H-D-Asp-OBzl-OH (600 mg, 2.69 mmol) in distilled water (10 ml), followed by the dropwise addition of 4-methyl-benzenesulfonyl chloride (614 mg, 3.22 mmol) in acetone (7 ml) then the reaction mixture was stirred at room temperature for 2 h at pH = 8. The acetone was removed under vacuum and the residue was extracted with NaHCO₃/diethyl ether (25 ml). The basic solution was acidified with solid NaHSO₄ to pH = 4–5 and extracted with ethyl acetate (3 × 20 ml). The combined organic phases were dried, filtered, and concentrated. The crude material was crystallized from ethyl acetate/diethyl ether and gave Tos-D-Asp-OBzl-OH (704 mg, 1.87 mmol, 69%). HRMS (EI) Calcd for C₁₈H₁₉NO₆S *m/z*: 378.1011 (M + H). Found: *m/z* 378.0949 (M + H). 1H NMR (500 MHz, DMSO-*d*₆) δ 7.79 (2H, d, *J* = 8 Hz), 7.47 (5H, m), 7.39 (2H, d, *J* = 8 Hz), 5.04 (2H, dd, *J* = 12 Hz), 4.33 (1H, dd, *J* = 7 Hz), 3.50 (1H, s), 3.44 (2H, t, *J* = 7 Hz), 2.84 (3H, s), 2.65 (1H, s).

(S)-N-(4-Amino-butyl)-2-(toluene-4-sulfonylamino)-succinamic acid cyclohexyl ester (4)

To a solution of Tos-Asp-OcHex-OH (103 mg, 0.28 mmol) in DMF (1 ml), DCC (64 mg, 0.31 mmol) and HOBT (42 mg, 0.31 mmol) were added and the reaction mixture was stirred for 30 min then DCU was filtered off. (4-Amino-butyl)-carbamic acid tert-butyl ester (52 mg, 0.28 mmol) was added to the solution and stirred for 4 h at room temperature. DMF was removed under vacuum and the residue was dissolved in ethyl acetate (20 ml), washed three times with saturated NaHSO₄, NaHCO₃ and brine, dried on Na₂SO₄, filtered and concentrated. The crude residue was dissolved in 50% TFA/DCM (5 ml), then the reaction mixture was stirred for 20 min at room temperature and then the solvent was removed. The crude product was purified by HPLC to give **4** (31 mg, 0.06 mmol, 25%). HRMS (EI) Calcd for C₂₁H₃₃N₃O₅S *m/z*: 440.2219 (M + H). Found: *m/z* 440.2171 (M + H). 1H NMR (500 MHz, DMSO-*d*₆) δ 8.11 (1H, t, *J* = 6 Hz), 7.78 (2H, d, *J* = 8 Hz), 7.50 (2H, d, *J* = 8 Hz), 4.56 (1H, s), 4.27 (1H, t, *J* = 7 Hz), 3.50 (2H, s), 3.12 (2H, m), 2.91 (2H, s), 2.62 (3H, s), 1.60 (8H, m), 1.33 (6H, m).

(S)-N-(6-Amino-hexyl)-2-(toluene-4-sulfonylamino)-succinamic acid cyclohexyl ester (5)

To a solution of Tos-Asp-OcHex-OH (101 mg, 0.27 mmol) in DMF (1 ml), DCC (64 mg, 0.31 mmol) and HOBT (21 mg, 0.31 mmol) were added and the reaction mixture was stirred for 30 min then DCU was filtered off. (6-Amino-hexyl)-carbamic acid tert-butyl ester (58 mg, 0.27 mmol) was added to the solution and stirred for 4 h at room temperature. DMF was removed under vacuum and the residue was dissolved in ethyl acetate (20 ml), washed three times with saturated NaHSO₄, NaHCO₃ and brine, dried on Na₂SO₄, filtered and concentrated. The crude residue was dissolved in 50% TFA/DCM (5 ml), then the reaction mixture was stirred for 20 min at room temperature and then the solvent was removed. The crude product was purified by HPLC to give **5** (35 mg, 0.07 mmol, 27%). HRMS (EI) Calcd for C₂₃H₃₇N₃O₅S *m/z*: 468.2532 (M + H). Found: *m/z* 468.2445 (M + H). 1H NMR (500 MHz, DMSO-*d*₆) δ 8.03 (1H, t, *J* = 6 Hz), 7.78 (2H, d, *J* = 8 Hz), 7.49 (2H, d, *J* = 8 Hz), 4.55 (1H, s), 4.27 (1H, dd, *J* = 7 Hz), 3.51 (2H, s), 3.10 (2H, m), 2.88 (2H, m), 2.63 (3H, s), 2.51 (3H, s), 1.65 (4H, m), 1.42 (14H, m).

(S)-N-(4-Guanidino-butyl)-2-(toluene-4-sulfonylamino)-succinamic acid cyclohexyl ester (6)

To a solution of Tos-Asp-OcHex-OH (340 mg, 0.92 mmol) in DMF (3 ml), HBTU (697 mg, 1.84 mmol) and HOBt (248 mg, 1.84 mmol) and DIEA (294 μ l, 1.84 mmol) were added. The above solution was added dropwise to the solution of agmatine sulphate (210 mg, 0.90 mmol) in aqueous NaHCO₃ (155 mg, 1.81 mmol in 2 ml water) then the reaction mixture was stirred at room temperature overnight. Solvents were removed under vacuum and the residue was dissolved in ethyl acetate (20 ml), washed three times with saturated NaHSO₄, NaHCO₃ and brine, dried on Na₂SO₄, filtrated and concentrated. The crude residue was purified by HPLC to give **6** (114 mg, 0.24 mmol, 26%). HRMS (EI) Calcd for C₂₃H₃₁N₅O₅S *m/z*: 490.2124 (M + H). Found: *m/z* 490.2129 (M + H). 1H NMR (500 MHz, DMSO-*d*₆) δ 8.06 (1H, t, *J* = 6 Hz), 7.75 (2H, d, *J* = 8 Hz), 7.47 (2H, d, *J* = 8 Hz), 4.52 (1H, s), 4.24 (1H, dd, *J* = 7 Hz), 3.50 (2H, s), 3.18 (2H, dd, *J* = 7 Hz), 2.61 (3H, s), 2.48 (5H, s), 1.65 (4H, t, *J* = 7 Hz), 1.49 (4H, m), 1.29 (6H, m).

(S)-N-(4-Guanidino-butyl)-2-(toluene-4-sulfonylamino)-succinamic acid benzyl ester (7)

To a solution of Tos-Asp-OBzl-OH (135 mg, 0.36 mmol) in DMF (2 ml), HBTU (137 mg, 0.36 mmol) and HOBt (48 mg, 0.36 mmol) and DIEA (58 μ l, 0.36 mmol) were added. The above solution was added dropwise to the solution of agmatine sulphate (91 mg, 0.39 mmol) in aqueous NaHCO₃ (60 mg, 0.70 mmol in 1 ml water) then the reaction mixture was stirred at room temperature overnight. Solvents were removed under vacuum and the residue was dissolved in ethyl acetate (20 ml), washed three times with saturated NaHSO₄, NaHCO₃ and brine, dried on Na₂SO₄, filtrated and concentrated. The crude residue was purified by HPLC to give **7** (25 mg, 0.05 mmol, 14%). HRMS (EI) Calcd for C₂₈H₃₆N₄O₅S *m/z*: 541.2484 (M + H). Found: *m/z* 541.2335 (M + H). 1H NMR (500 MHz, DMSO-*d*₆) δ 8.42 (1H, t, *J* = 5 Hz), 8.09 (2H, d, *J* = 8 Hz), 7.79 (5H, m), 7.69 (2H, d, *J* = 8 Hz), 5.33 (2H, q, *J* = 12 Hz), 4.69 (1H, dd, *J* = 7 Hz), 3.82 (2H, s), 3.51 (2H, m), 3.42 (2H, dd, *J* = 7 Hz), 2.96 (3H, s), 2.81 (5H, m), 1.83 (4H, m).

(R)-N-(4-Guanidino-butyl)-2-(toluene-4-sulfonylamino)-succinamic acid benzyl ester (8)

To a solution of Tos-D-Asp-OBzl-OH (135 mg, 0.36 mmol) in DMF (2 ml), HBTU (272 mg, 0.72 mmol) and HOBt (96 mg, 0.72 mmol) and DIEA (116 μ l, 0.72 mmol) were added. The above solution was added dropwise to the solution of agmatine sulphate (91 mg, 0.39 mmol) in aqueous NaHCO₃ (60 mg, 0.70 mmol in 1 ml water) then the reaction mixture was stirred at room temperature overnight. Solvents were removed under vacuum and the residue was dissolved in ethyl acetate (20 ml), washed three times with saturated NaHSO₄, NaHCO₃ and brine, dried on Na₂SO₄, filtrated and concentrated. The crude residue was purified by HPLC to give **8** (45 mg, 0.09 mmol, 26%). HRMS (EI) Calcd for C₂₂H₃₅N₅O₅S *m/z*: 482.2437 (M + H). Found: *m/z* 482.2398 (M + H). 1H NMR (500 MHz, DMSO-*d*₆) δ 8.41 (1H, t, *J* = 5 Hz), 8.07 (2H, d, *J* = 8 Hz), 7.76 (5H, m), 7.67 (2H, d, *J* = 8 Hz), 5.31 (2H, q, *J* = 12 Hz), 4.68 (1H, dd, *J* = 7 Hz), 3.79 (2H, s), 3.50 (2H, dd, *J* = 7 Hz), 3.40 (2H, dd, *J* = 7 Hz), 2.94 (3H, s), 2.79 (5H, m), 1.82 (4H, m).

(S)-N¹-Cyclohexyl-N⁴-{2-[4-(4,5-dihydro-1H-imidazol-2-yl)-phenyl]-ethyl}-2-(toluene-4-sulfonylamino)-succinamide (9)

To a solution of Tos-Asp-OcHex-OH (25 mg, 0.068 mmol) in DMF (500 μ l), HBTU (26 mg, 0.068 mmol) and HOBt (9 mg, 0.068 mmol)

and DIEA (11 μ l, 0.068 mmol) were added and the reaction mixture was stirred for 15 min then 2-[4-(4,5-Dihydro-1H-imidazol-2-yl)-phenyl]-ethylamine dihydro-chloride (23 mg, 0.088 mmol) was added to the solution and stirred for 4 h at room temperature. DMF was removed under vacuum and the residue was dissolved in ethyl acetate (20 ml), washed three times with saturated NaHSO₄, saturated NaHCO₃ and once with brine, dried with Na₂SO₄, filtered and concentrated. The crude residue was purified by HPLC to give **9** (14 mg, 39%). HRMS (EI) Calcd for C₂₁H₃₃N₃O₅S *m/z*: 440.2219 (M + H). Found: *m/z* 440.2212 (M + H). 1H NMR (500 MHz, DMSO-*d*₆) δ 8.22 (1H, s), 8.01 (2H, d, *J* = 8 Hz), 7.80 (2H, d, *J* = 8 Hz), 7.64 (2H, d, *J* = 8 Hz), 7.51 (2H, d, *J* = 8 Hz), 4.57 (1H, s), 4.28 (1H, dd, *J* = 7 Hz), 4.15 (2H, s), 3.51 (2H, s), 3.40 (2H, m), 2.92 (3H, t, *J* = 7 Hz), 2.65 (5H, s), 2.47 (2H, m), 1.69 (4H, m), 1.34 (6H, m).

(S)-N-{2-[4-(4,5-Dihydro-1H-imidazol-2-yl)-phenyl]-ethyl}-2-(toluene-4-sulfonylamino)-succinamic acid benzyl ester (10)

To a solution of Tos-Asp-OBzl-OH (40 mg, 0.106 mmol) in DMF (500 μ l), HBTU (80 mg, 0.212 mmol) and HOBt (29 mg, 0.212 mmol) and DIEA (34 μ l, 0.212 mmol) were added and the reaction mixture was stirred for 15 min then 2-[4-(4,5-Dihydro-1H-imidazol-2-yl)-phenyl]-ethylamine dihydro-chloride (26 mg, 0.127 mmol) was added to the solution and stirred for 4 h at room temperature. DMF was removed under vacuum and the residue was dissolved in ethyl acetate (20 ml), washed three times with saturated NaHSO₄, saturated NaHCO₃ and once with brine, dried with Na₂SO₄, filtered and concentrated. The crude residue was purified by HPLC to give **10** (40 mg, 69%). HRMS (EI) Calcd for C₂₃H₃₇N₃O₅S *m/z*: 468.2532 (M + H). Found: *m/z* 468.2493 (M + H). 1H NMR (500 MHz, DMSO-*d*₆) δ 8.44 (1H, t, *J* = 5 Hz), 8.19 (2H, d, *J* = 8 Hz), 7.98 (2H, d, *J* = 8 Hz), 7.80 (2H, d, *J* = 8 Hz), 7.68 (5H, m), 7.58 (2H, d, *J* = 8 Hz), 5.20 (2H, m), 4.58 (1H, dd, *J* = 7 Hz), 4.34 (2H, s), 3.71 (2H, s), 3.58 (2H, m), 3.09 (2H, t, *J* = 7 Hz), 2.87 (5H, m), 2.69 (2H, m).

(R)-N-{2-[4-(4,5-Dihydro-1H-imidazol-2-yl)-phenyl]-ethyl}-2-(toluene-4-sulfonylamino)-succinamic acid benzyl ester (11)

To a solution of Tos-D-Asp-OBzl-OH (37 mg, 0.098 mmol) in DMF (500 μ l), HBTU (52 mg, 0.136 mmol) and HOBt (18 mg, 0.136 mmol) and DIEA (22 μ l, 0.136 mmol) were added and the reaction mixture was stirred for 15 min then 2-[4-(4,5-Dihydro-1H-imidazol-2-yl)-phenyl]-ethylamine dihydro-chloride (26 mg, 0.098 mmol) was added to the solution and stirred for 4 h at room temperature. DMF was removed under vacuum and the residue was dissolved in ethyl acetate (20 ml), washed three times with saturated NaHSO₄, saturated NaHCO₃ and once with brine, dried with Na₂SO₄, filtered and concentrated. The crude residue was purified by HPLC to give **11** (36 mg, 67%). HRMS (EI) Calcd for C₂₃H₃₁N₅O₅S *m/z*: 490.2124 (M + H). Found: *m/z* 490.2140 (M + H). 1H NMR (500 MHz, DMSO-*d*₆) δ 8.45 (1H, t, *J* = 5 Hz), 8.21 (2H, d, *J* = 8 Hz), 7.99 (2H, d, *J* = 8 Hz), 7.82 (2H, d, *J* = 8 Hz), 7.70 (5H, m), 7.59 (2H, d, *J* = 8 Hz), 5.23 (2H, m), 5.13 (2H, m), 4.60 (1H, dd, *J* = 7 Hz), 4.36 (2H, s), 3.72 (2H, s), 3.58 (2H, m), 3.09 (2H, t, *J* = 7 Hz), 2.87 (3H, s), 2.72 (2H, m).

Tos-Asp-(OcHex)-OH (12)

NaHCO₃ (1.680 g, 20.00 mmol) was added to a solution of H-Asp-(OcHex)-OH (2.150 g, 10.00 mmol) in distilled water (30 ml), followed by the dropwise addition of 4-methyl-benzenesulfonyl chloride (2.100 g, 11.01 mmol) in acetone (20 ml) then the reaction mixture was stirred at room temperature for 4 h at pH = 8. The acetone was removed under vacuum and the residue was

extracted with NaHCO₃/diethyl ether (25 ml). The basic solution was acidified with solid NaHSO₄ to pH = 4–5 and extracted with ethyl acetate (3 × 20 ml). The combined organic phases were dried, filtered, and concentrated. The crude product was crystallized from hexane/diethyl ether and gave Tos-Asp-(OcHex)-OH (1.918 g, 5.19 mmol, 47%). HRMS (EI) Calcd for C₁₇H₂₃NO₆S *m/z*: 370.1324 (M + H). Found: *m/z* 370.1232 (M + H). ¹H NMR (500 MHz, DMSO-*d*₆) δ 7.80 (2H, d, *J* = 8 Hz), 7.50 (2H, d, *J* = 8 Hz), 4.70 (1H, m), 4.22 (1H, q, *J* = 7 Hz), 3.52 (1H, s), 2.74 (3H, m), 2.63 (3H, s), 1.83 (4H, m), 1.40 (6H, m).

Tos-D-Asp-(OBzl)-OH (13)

NaHCO₃ (336 mg, 4.00 mmol) was added to a solution of H-Asp-(OcHex)-OH (430.5 mg, 2.00 mmol) in distilled water (10 ml), followed by the dropwise addition of 4-methyl-benzenesulfonyl chloride (432 mg, 2.27 mmol) in acetone (10 ml) then the reaction mixture was stirred at room temperature for overnight at pH = 8. The acetone was removed under vacuum and the residue was extracted with NaHCO₃/diethyl ether (25 ml). The basic solution was acidified with solid NaHSO₄ to pH = 4–5 and extracted with ethyl acetate (3 × 20 ml). The combined organic phases were dried, filtered, and concentrated. The crude product was crystallized from hexane/diethyl ether and gave Tos-Asp-(OcHex)-OH (710 mg, 1.880 mmol, 93%). HRMS (EI) Calcd for C₁₈H₁₉NO₆S *m/z*: 378.1011 (M + H). Found: *m/z* 378.0909 (M + H). ¹H NMR (500 MHz, DMSO-*d*₆) δ 7.76 (2H, d, *J* = 8 Hz), 7.41 (2H, d, *J* = 8 Hz), 7.26 (5H, m), 5.49 (2H, t, *J* = 7 Hz), 3.79 (1H, m), 3.49 (1H, s), 3.42 (2H, t, *J* = 7 Hz), 2.80 (3H, m), 2.65 (1H, s).

(S)-N-(4-Amino-butyl)-3-(toluene-4-sulfonylamino)-succinamic acid cyclohexyl ester (14)

To a solution of Tos-Asp-(OcHex)-OH (100 mg, 0.27 mmol) in DMF (1 ml), DCC (64 mg, 0.31 mmol) and HOBt (42 mg, 0.31 mmol) were added and the reaction mixture was stirred for 30 min then DCU was filtered off. (4-Amino-butyl)-carbamic acid tert-butyl ester (52 mg, 0.28 mmol) was added to the solution and stirred for 4 h at room temperature. DMF was removed under vacuum and the residue was dissolved in ethyl acetate (20 ml), washed three times with saturated NaHSO₄, NaHCO₃ and brine, dried on Na₂SO₄, filtered and concentrated. The crude residue was dissolved in 50% TFA/DCM (5 ml), then the reaction mixture was stirred for 20 min at room temperature and then the solvent was removed. The crude product was purified by HPLC to give **14** (51 mg, 0.09 mmol, 35%). HRMS (EI) Calcd for C₂₉H₃₂N₄O₅S *m/z*: 549.2171 (M + H). Found: *m/z* 549.2182 (M + H). ¹H NMR (500 MHz, DMSO-*d*₆) δ 8.10 (1H, t, *J* = 6 Hz), 7.80 (2H, d, *J* = 8 Hz), 7.50 (2H, d, *J* = 8 Hz), 4.67 (1H, s), 4.18 (1H, t, *J* = 7 Hz), 3.50 (2H, s), 3.02 (2H, m), 2.89 (2H, s), 2.65 (3H, s), 2.52 (3H, s), 1.81 (4H, m), 1.48 (10H, m).

(S)-N-(7-Amino-heptyl)-3-(toluene-4-sulfonylamino)-succinamic acid cyclohexyl ester (15)

To a solution of Tos-Asp-(OcHex)-OH (100 mg, 0.27 mmol) in DMF (1 ml), DCC (64 mg, 0.31 mmol) and HOBt (21 mg, 0.31 mmol) were added and the reaction mixture was stirred for 30 min then DCU was filtered off. (6-Amino-hexyl)-carbamic acid tert-butyl ester (58 mg, 0.28 mmol) was added to the solution and stirred for 4 h at room temperature. DMF was removed under vacuum and the residue was dissolved in ethyl acetate (20 ml), washed three times with saturated NaHSO₄, NaHCO₃ and brine, dried on Na₂SO₄, filtered and concentrated. The crude residue was dissolved in 50%

TFA/DCM (5 ml), then the reaction mixture was stirred for 20 min at room temperature and then the solvent was removed. The crude product was purified by HPLC to give **15** (58 mg, 0.10 mmol, 38%). HRMS (EI) Calcd for C₂₉H₃₂N₄O₅S *m/z*: 549.2171 (M + H). Found: *m/z* 549.2180 (M + H). ¹H NMR (500 MHz, DMSO-*d*₆) δ 8.02 (1H, t, *J* = 6 Hz), 7.81 (2H, d, *J* = 8 Hz), 7.51 (2H, d, *J* = 8 Hz), 4.69 (1H, s), 4.2 (1H, dd, *J* = 7 Hz), 3.55 (2H, s), 2.99 (2H, m), 2.93 (2H, m), 2.67 (3H, s), 2.53 (3H, s), 1.82 (4H, m), 1.66 (6H, m), 1.38 (8H, m).

(S)-N-{2-[4-(4,5-Dihydro-1H-imidazol-2-yl)-phenyl]-ethyl}-3-(toluene-4-sulfonylamino)-succinamic acid cyclohexyl ester (16)

To a solution of Tos-Asp-(OcHex)-OH (56 mg, 0.15 mmol) in DMF (1 ml), HBTU (114 mg, 0.30 mmol) and HOBt (41 mg, 0.30 mmol) and DIEA (48 μL, 0.30 mmol) were added and the reaction mixture was stirred for 15 min then 2-[4-(4,5-Dihydro-1H-imidazol-2-yl)-phenyl]-ethylamine dihydro-chloride (40 mg, 0.12 mmol) was added to the solution and stirred for 4 h at room temperature. DMF was removed under vacuum and the residue was dissolved in ethyl acetate (20 ml), washed three times with saturated NaHSO₄, saturated NaHCO₃ and once with brine, dried with Na₂SO₄, filtered and concentrated. The crude residue was purified by HPLC to give **16** (48 mg, 0.09 mmol, 58%). HRMS (EI) Calcd for C₂₈H₃₆N₄O₅S *m/z*: 541.2484 (M + H). Found: *m/z* 541.2285 (M + H). ¹H NMR (500 MHz, DMSO-*d*₆) δ 8.22 (1H, t, 5 Hz), 8.01 (2H, d, *J* = 8 Hz), 7.82 (2H, d, *J* = 8 Hz), 7.59 (2H, d, *J* = 8 Hz), 7.52 (2H, d, *J* = 8 Hz), 4.68 (1H, s), 4.20 (1H, dd, *J* = 5 Hz), 4.12 (2H, s), 3.52 (2H, s), 3.30 (2H, m), 2.83 (2H, m), 2.67 (5H, s), 2.52 (2H, s), 1.82 (4H, m), 1.39 (6H, m).

(R)-N-{2-[4-(4,5-Dihydro-1H-imidazol-2-yl)-phenyl]-ethyl}-3-(toluene-4-sulfonylamino)-succinamic acid benzyl ester (17)

To a solution of Tos-D-Asp-(OBzl)-OH (50 mg, 0.13 mmol) in DMF (1 ml), HBTU (100 mg, 0.26 mmol) and HOBt (36 mg, 0.26 mmol) and DIEA (42 μL, 0.26 mmol) were added and the reaction mixture was stirred for 15 min then 2-[4-(4,5-Dihydro-1H-imidazol-2-yl)-phenyl]-ethylamine dihydro-chloride (51 mg, 0.19 mmol) was added to the solution and stirred for 4 h at room temperature. DMF was removed under vacuum and the residue was dissolved in ethyl acetate (20 ml), washed three times with saturated NaHSO₄, saturated NaHCO₃ and once with brine, dried with Na₂SO₄, filtered and concentrated. The crude residue was purified by HPLC to give **17** (38 mg, 0.07 mmol, 52%). HRMS (EI) Calcd for C₂₉H₃₂N₄O₅S *m/z*: 549.2171 (M + H). Found: *m/z* 549.2156 (M + H). ¹H NMR (500 MHz, DMSO-*d*₆) δ 8.43 (1H, t, *J* = 5 Hz), 8.19 (2H, d, *J* = 8 Hz), 7.99 (2H, d, *J* = 8 Hz), 7.78 (2H, d, *J* = 8 Hz), 7.66 (7H, m), 5.30 (2H, dd, 15 Hz), 4.40 (1H, dd, *J* = 7 Hz), 4.35 (2H, s), 3.86 (2H, s), 3.46 (2H, m), 3.00 (2H, t, *J* = 7 Hz), 2.88 (5H, s), 2.70 (2H, m).

Acknowledgement

The authors thank for the NMR measurements to Dr Péter Forgó and for accurate mass determination to Dr Zoltán Szabó.

References

- Ritchie TJ, Dziadulewicz EK, Culshaw AJ, Müller W, Burgess GM, Bloomfield GC, Drake GS, Dunstan AR, Beattie D, Hughes GA, Ganju P, McIntyre P, Bevan SJ, Davis C, Yaqoob M. Potent and orally bioavailable non-peptide antagonists at the human bradykinin B₁ receptor based on a 2-alkylamino-5-sulfamoylbenzamide core. *J. Med. Chem.* 2004; **47**: 4642–4644.

2. Couture R, Harrisson M, Vianna RM, Cloutier F. Kinin receptors in pain and inflammation. *Eur. J. Pharmacol.* 2001; **429**: 161–176.
3. Bhoola KD, Figueroa CD, Worthy K. Bioregulation of kinins: kallikreins, kininogens, and kininases. *Pharmacol. Rev.* 1992; **44**: 1–80.
4. Dziadulewicz EK, Ritchie TJ, Hallett A, Snell CR, Davies JW, Wrigglesworth R, Dunstan AR, Bloomfield GC, Drake GS, McIntyre P, Brown MC, Burgess GM, Lee W, Davis C, Yaqoob M, Phagoo SB, Phillips E, Perkins MN, Campbell EA, Davis AJ, Rang HP. Nonpeptide bradykinin B₂ receptor antagonists: conversion of rodent-selective bradyzide analogues into potent, orally-active human bradykinin B₂ receptor antagonists. *J. Med. Chem.* 2002; **45**: 2160–2172.
5. Regoli D, Barabe J. Pharmacology of bradykinin and related kinins. *Pharmacol. Rev.* 1980; **32**: 1–46.
6. Farmer SG. In *The Kinin System*. Academic Press: London, 1997.
7. Palczewski K, Kumasaka T, Hori T, Behnke CA, Motoshima H, Fox BA, Le Trong I, Teller DC, Okada T, Stenkamp RE, Yamamoto M, Miyano M. Crystal structure of rhodopsin: a G protein-coupled receptor. *Science* 2000; **289**: 739–745.
8. Rasmussen SGF, Choi HJ, Rosenbaum DM, Kobilka TS, Thian FS, Edwards PC, Burghammer M, Ratnala VR, Sanishvili R, Fischetti RF, Schertler GF, Weis WI, Kobilka BK. Crystal structure of the human β 2 adrenergic G-protein-coupled receptor. *Nature* 2007; **450**: 383–387.
9. Cherezov V, Rosenbaum DM, Hanson MA, Rasmussen SGF, Thian FS, Kobilka TS, Choi HJ, Kuhn P, Weis WI, Kobilka BK, Stevens RC. High-resolution crystal structure of an engineered human β 2-adrenergic G protein coupled receptor. *Science* 2007; **318**: 1258–1265.
10. Marceau F, Hess JF, Bachvarov DR. The B₁ Receptors for Kinins. *Pharmacol. Rev.* 1998; **50**: 357–386.
11. Phagoo SB, Poole S, Leeb-Lundberg LMF. Autoregulation of bradykinin receptors: agonists in the presence of interleukin-1 β shift the repertoire of receptor subtypes from B₂ to B₁ in human lung fibroblast. *Mol. Pharmacol.* 1999; **56**: 325–333.
12. Rashid MH, Inoue M, Matsumoto M, Ueda H. Switching of bradykinin-mediated nociception following partial sciatic nerve injury in mice. *J. Pharmacol. Exp. Ther.* 2004; **308**: 1158–1164.
13. Siebeck M, Schorr M, Spannagl E, Lechner M, Fritz H, Cheronis JC, Whalley ET. B₁ kinin receptor activity in pigs is associated with pre-existing infection. *Immunopharmacology* 1998; **40**: 49–55.
14. Hara DB, Leite DF, Fernandes ES, Passos GF, Guimarães AO, Pesquero JB, Campos MM, Calixto JB. The relevance of kinin B₁ receptor upregulation in a mouse model of colitis. *Br. J. Pharmacol.* 2008; **154**: 1276–1286.
15. Stadnicki A, Pastucha E, Nowaczyk G, Mazurek U, Plewka D, Machnik G, Wilczok T, Colman RW. Immunolocalization and expression of kinin B₁R and B₂R receptors in human inflammatory bowel disease. *Am. J. Physiol. Gastrointest. Liver Physiol.* 2005; **289**: 361–366.
16. Duchene J, Ahluwalia A. The kinin B₁ receptor and inflammation: new therapeutic target for cardiovascular disease. accepted in *Curr. Opin. Pharmacol.* 2009; (in press). DOI:10.1016/j.coph.2008.11.011.
17. Belichard P, Landry M, Faye P, Bachvarov DR, Bouthillier J, Pruneau D, Marceau F. Inflammatory hyperalgesia induced by zymosan in the plantar tissue of the rat: effect of kinin receptor antagonists. *Immunopharmacology* 2000; **46**: 139–147.
18. Rupniak NMJ, Boyce S, Webb JK, Williams AR, Carlson EJ, Hill RG, Borkowski JA, Hess JF. Effects of the bradykinin B₁ receptor antagonist des-Arg⁹[Leu⁸]bradykinin and genetic disruption of the B₂ receptor on nociception in rats and mice. *Pain* 1997; **71**: 89–97.
19. Regoli D, Allogho SN, Rizzi A, Gobeil FJ. Bradykinin receptors and their antagonists. *Eur. J. Pharmacol.* 1998; **348**: 1–10.
20. Stewart JM, Gera L, York EJ, Chan DC, Whalley EJ, Bunn PA, Vavrek R. Metabolism-resistant bradykinin antagonists: development and applications. *Biol. Chem.* 2001; **382**: 37–41.
21. Regoli D, Barabe J, Park WK. Receptors for bradykinin in rabbit aortae. *Can. J. Physiol. Pharmacol.* 1977; **55**: 855–867.
22. Pellegrini M, Tancredi M, Ravero P, Mierke DF. Probing the topological arrangement of the N- and C-terminal residues of bradykinin for agonist activity at the B₁ receptor. *J. Med. Chem.* 1999; **42**: 3369–3377.
23. Su DS, Markowitz MK, DiPardo RM, Murphy KL, Harrell CM, O'Malley SS, Ransom RW, Chang RSL, Ha S, Hess FJ, Pettibone DJ, Mason GS, Boyce S, Freidinger RM, Bock MG. Discovery of a potent, non-peptide bradykinin B₁ receptor antagonist. *J. Am. Chem. Soc.* 2003; **125**: 7516–7517.
24. Amblard M, Daffix I, Bedos P, Berge G, Pruneau D, Paquet J-L, Luc-carini J-M, Be'lichard P, Dodey P, Martinez J. Design and synthesis of potent bradykinin agonists containing a benzothiazepine moiety. *J. Med. Chem.* 1999; **42**: 4185–4192.
25. Bock MG, Hess JF, Pettibone DJ. Chapter 12. Bradykinin-1 receptor antagonists. *Annu. Rep. Med. Chem.* 2003; **38**: 111–120.
26. Bock MG, Longmore J. Bradykinin antagonists: new opportunities. *Curr. Opin. Chem. Biol.* 2000; **4**: 401–406.
27. Gougat J, Ferrari B, Sarran L, Planchenault C, Poncelet M, Maruani J, Alonso R, Cudennec A, Croci T, Guagnini F, Urban-Szabo K, Martinolle JP, Soubrié P, Finance O, Le Fur GG. SSR240612 [(2R)-2-[[[(3R)-3-(1,3-Benzodioxol-5-yl)-3-[[[(6-methoxy-2-naphthyl)sulfonyl]amino]propanoyl]amino]-3-(4-[[[2R,6S)-2,6-dimethylpiperidinyl]methyl]phenyl]-N-isopropyl-N-methylpropanamide hydrochloride], a new nonpeptide antagonist of the bradykinin B₁ receptor: biochemical and pharmacological characterization. *J. Pharmacol. Exp. Ther.* 2004; **309**: 661–669.
28. Horlick RA, Ohlmeyer MH, Stroke IL, Strohl B, Pan G, Schilling AE, Paradkar V, Quintero JG, You M, Riviello C, Thorn MB, Damaj B, Fitzpatrick VD, Dolle RE, Webb ML, Baldwin JJ, Sigal NH. Small molecule antagonists of the bradykinin B₁ receptor. *Immunopharmacology* 1999; **43**: 169–177.
29. Wood MR, Kim JJ, Han W, Dorsey BD, Homnick CF, DiPardo RM, Kuduk SD, MacNeil T, Murphy KL, Lis EV, Ransom RW, Stump GL, Lynch JJ, O'Malley SS, Miller PJ, Chen TB, Harrell CM, Chang RSL, Sandhu P, Ellis JD, Bondiskey PJ, Pettibone DJ, Freidinger RM, Bock MG. Benzodiazepines as potent and selective bradykinin B₁ antagonists. *J. Med. Chem.* 2003; **46**: 1803–1806.
30. Ransom RW, Harrell CM, Reiss DR, Murphy KL, Chang RSL, Hess JF, Miller PJ, O'Malley SS, Hey PJ, Kunapuli P, Su DS, Markowitz MK, Wallace MA, Raab CE, Jones AN, Dean DC, Pettibone DJ, Freidinger RM, Bock MG. Pharmacological characterization and radioligand binding properties of a high-affinity, nonpeptide, bradykinin B₁ receptor antagonist. *Eur. J. Pharmacol.* 2004; **499**: 77–84.
31. Kuduk SD, Ng C, Feng DM, Wai JMC, Chang RSL, Harrell CM, Murphy KL, Ransom RW, Reiss DR, Ivarsson M, Mason G, Boyce S, Tang C, Prueksaritanont T, Freidinger RM, Pettibone DJ, Bock MG. 2,3-Diaminopyridine bradykinin B₁ receptor antagonists. *J. Med. Chem.* 2004; **47**: 6439–6442.
32. Su DS, Markowitz MK, Murphy KL, Wan BL, Zrada MM, Harrell CM, O'Malley SS, Hess FJ, Ransom RW, Chang RS, Wallace MA, Raab CE, Dean DC, Pettibone DJ, Freidinger RM, Bock MG. Development of an efficient and selective radioligand for bradykinin B₁ receptor occupancy studies. *Bioorg. Med. Chem. Lett.* 2004; **14**: 6045–6048.
33. Ha SN, Hey PJ, Ransom RW, Harrell CM Jr, Murphy KL, Chang R, Chen TB, Su DS, Markowitz MK, Bock MG, Freidinger RM, Hess FJ. Binding modes of dihydroquinoxalinones in a homology model of bradykinin receptor 1. *Biochem. Biophys. Res. Commun.* 2005; **331**(1): 159–166.
34. Ranganathan R. Signalling across the cell membrane. *Science* 2007; **318**: 1253–1254.
35. Massotte D, Kieffer BL. The second extracellular loop: a damper for G protein-coupled receptors? *Nat. Struct. Mol. Biol.* 2005; **12**: 287–288.
36. Ha SN, Hey PJ, Ransom RW, Bock MG, Su DS, Murphy KL, Chang R, Chen TB, Pettibone D, Hess JF. Identification of the critical residues of bradykinin receptor B₁ for interaction with the kinins guided by site-directed mutagenesis and molecular modeling. *Biochemistry* 2006; **45**: 14355–14361.
37. Šali A, Blundell TL. Comparative protein modelling by satisfaction of spatial restraints. *J. Mol. Biol.* 1993; **234**: 779–815.
38. Hanson MA, Cherezov V, Griffith MT, Roth CB, Jaakola VP, Chien EY, Velasquez J, Kuhn P, Stevens C. A Specific cholesterol binding site is established by the 2.8 Å structure of the human beta(2)-adrenergic receptor. *Structure* 2008; **16**: 897.
39. SYBYL 7.3, Tripos International, 1699 South Hanley Rd., St. Louis, Missouri, 63144, USA.
40. Ballesteros, JA, Weinstein H. Integrated methods for the construction of three-dimensional models and computational probing of structure-function relations in G protein-coupled receptors. *Methods Neurosci.* 1995; **25**: 366–428.